ISSN: 2319-8753

International Journal of Innovative Research in Science, Engineering and Technology

(An ISO 3297: 2007 Certified Organization)

Vol. 2, Issue 9, September 2013

THEORETICAL INVESTIGATION OF THE STRUCTURAL, ELECTRONIC, ELASTIC, AND OPTICAL PROPERTIES OF ZINC-BLENDE BeS UNDER HIGH PRESSURE

BadalH.Elias

Faculty of Science, School of Physics, Duhok University,Duhok, Iraq

Abstract:A theoretical study of structural, electronic, elastic and optical properties of zinc-blende BeS under hydrostatic pressure is presented using ab-initio plane wave pseudopotential density functional theory method within the local density approximation (LDA) and generalized gradient approximation (GGA) .The dependencies of the elastic constants, the bulk modulus, young modulus and energy gaps on the applied pressure are presented, and the results are in good agreement with comparable experimental and theoretical values. Also the energy band structure and density of states under high pressure have been analysed. Furthermore, the optical constant, including the dielectric function, optical reflectivity, refractive index, optical conductivity and electron energy loss, are discussed for radiation up to 50 e V.

Keywords:BeS, Electronic structure, Optical properties, First principles calculations, Elastic properties, Zinc-blende structure.

I. INTRODUCTION

Recently, it has become possible to compute with a great accuracy an important number of electronic and structural properties of solids from first-principles calculations. This kind of development in computer simulations has opened up many of interesting and existing possibilities in condensed matter studies. For example, it is now possible to explain and to predict properties of solids which were previously inaccessible to experiments .The II–VI semiconductors compounds have been extensively studied in recent years because of their scientific and technology interests.They are used in the fabrication of light-emitting devices that are employed in optical processing, detection systems for environmental pollution andcolor-displaying modules. In particular, the beryllium chalcogenidesBeS, BeSe and BeTe are the II–VI compounds that crystallize in the fourfoldcoordinated zinc-blende (B3) structure at low pressure. These BeX (X = S, Se and Te) compounds have structure and binding similar to those of the III-P group of semiconductors. They have large band gaps (2.7–5.5 eV) and a high value of the bulk modulus (B) that results in an increased hardness, and stability [1, 2]. Experimental studies on BeX (X = S, Se and Te) compounds are less frequently reported probably because of its high degree of toxic nature. The pioneering works by Yim et al. [3], Zachariasen [4], Narayana et al. [5] and Luo et al. [6] were focused on the structural phase transformation and showed that there exists a structural phase transition from the zinc-blend (B3) to NiAs(B8) for these compounds. On the theoretical side, the ab-initio calculations have been extensively used to obtain the structural [7–15], electronic [12–19], elastic [12, 13, 16, 17], lattice dynamical [21–24], thermodynamic [25-27], optical [12, 14,16,18,29, 30] properties for beryllium chalcogenides and their alloys [31–35].

BeS is an interesting material with high hardness. It belongs to the beryllium chalcogenides family and crystallizes under normal conditions with the zinc-blende structure. Under high pressure, the first-principles calculation of Muñoz et al. [36]showed that BeS experiences a phase transition to the nickel arsenide (NiAs) structure. This prediction has been confirmed by the experimental studies of Narayana et al. [5]who reported the existence of a reversible first-order phase transition of BeS from the zinc-blende structure, to the nickel–arsenide structure.

The present work is undertaken to study the structure, electronic, elastic and optical properties of zinc-blendBeS under pressure from first principlescalculations. To investigate these properties, we performed ab-initio pseudopotential calculations with the local density approximation (LDA) and generalized gradient approximation (GGA) of the density functional theory (DFT).

ISSN: 2319-8753

International Journal of Innovative Research in Science, Engineering and Technology

(An ISO 3297: 2007 Certified Organization)

Vol. 2, Issue 9, September 2013

The rest of the paper is organized as follows. In Section II, we brieflydescribe the theoretical method used in the presentwork. Results and discussion are presented in Section III. A summary of the work is given in Section IV.

II. THEORETICAL METHOD

A. *Total energy electronic structure calculations*

The calculations were performed using the Cambridge Series of Total Energy Package (CASTEP) [37-42] code in the framework of density functional theory DFT using Vanderbilt-type ultra-soft pseudopotential [39]for the electron-ion interactions. The exchange-correlational potential of Ceperley and Alder [40] as parameterized by Perdew and Zunger [41] (CAPZ) in local densityapproximation (LDA), and the generalized gradient approximation (GGA) schemes of Perdew-Burke-Ernzerhof [42] (PBE). The electronic wave functions are expanded in a plane wave basis set with cut-off energy of 250 eV. Pseudo-atom calculations are performed for S $3s^2 3p^4$ and Be $2s^2$. For the Brillion-zone k-point sampling, we use the Monkhorst-Pack mesh with 4 × 4 × 4 k-points. These parameters are sufficient in leading to well converged total energy, geometrical configurations and elastic stiffness coefficients.

Geometry optimization was conducted using convergence thresholds of 1×10^{-5}eV $atom^{-1}$ for the total energy, 0.03 eV$Å^{-1}$ for the maximum force, 0.05 GPa for maximum stress and 0.001Å for maximum displacement.

B. *Elastic constants*

The elastic constants of solids provide a link between the mechanical and dynamical behaviors of crystals, and give important information concerning the nature of the forces operating in solids. For a cubic lattice, there are three independent components, C_{11}, C_{12} and C_{44}. Therefore, we need only a set of three equations to calculate these three constants. This implies that only three types of strain must be applied to the crystal structure. The equation of state directly yields the behavior under isotropicvolumetric strain and hence it can be used to determine the bulk modulusB,of the crystals. For a cubic crystal, the bulk modulus is defined as $B=(C_{11}+2C_{12})/3$ [43].

A second relationship between C_{11} and C_{12} can be obtained by applying a volume conserving tetragonal strain tensor. The shear elastic constant, $C_S=(C_{11}-C_{12})/2$,the strain tensor is given by [49].

$$\varepsilon=\begin{pmatrix}\delta & 0 & 0\\ 0 & -\delta & 0\\ 0 & 0 & \delta^2/(1-\delta^2)\end{pmatrix} \quad (1)$$

Here, δ is the deformation parameter. Under the tetragonal shear strain. The total energy of the system is given by;

$$E(\delta)=E_0+2C_sV_0\delta^2+O(\delta^4) \quad (2)$$

Here, E_0 is the energy of unstrained state, C_S is the cubic shear constant and V_0 is the zero strain volume. A parabolic fit to the strain energy versus strain δ^2 yields the value of shear elastic constant. The strain tensor:

$$\varepsilon=\begin{pmatrix}0 & \delta/2 & 0\\ \delta/2 & 0 & 0\\ 0 & 0 & \delta^2/(4-\delta^2)\end{pmatrix} \quad (3)$$

was applied to determine the pure shear elastic constant, C_{44}, it yields the total energy.

$$E(\delta)=E_0+\frac{1}{2}C_{44}V_0\delta^2+O(\delta^4) \quad (4)$$

Kleinmann parameter, which is an important parameter describing the relative positions of the cation and anion sublattices. is given by [49]:

ISSN: 2319-8753

International Journal of Innovative Research in Science, Engineering and Technology

(An ISO 3297: 2007 Certified Organization)

Vol. 2, Issue 9, September 2013

$$\xi = \frac{C_{11} + 8C_{12}}{7C_{11} + 2C_{12}} \quad (5)$$

Shear modulus is given by the expression;

$$G = \frac{G_V + G_R}{2} \quad (6)$$

Where G_R is Reuss modulus given by;

$$G_R = \frac{5(C_{11} - C_{12})C_{44}}{4C_{44} + 3(C_{11} - C_{12})} \quad (7)$$

and G_v the Voight modulus, is defined as;

$$G_V = \frac{1}{5}(3C_{44} + C_{11} - C_{12}) \quad (8)$$

The Young modulus E and Poisson ratio γ are related to the hardness for polycrystalline materials and they are given by [8];

$$E = \frac{9BG}{3B+G} \quad (9)$$

and

$$\gamma = \frac{1}{2}\left(\frac{3B-E}{3B}\right) \quad (10)$$

C. Optical properties

The study of the optical functions helps to give a better understanding of the electronic structure. One of such functions the complex dielectric function, $\varepsilon(\omega) = \varepsilon_1(\omega) + i\varepsilon_2(\omega)$. The imaginary part $\varepsilon_2(\omega)$ is obtained from the momentum matrix elements between the occupied and the unoccupied electronic states and calculated directly using: [44]

$$\varepsilon_2(\omega) = \frac{e^2\hbar}{\pi m^2\omega^2}\sum_{v,c}\int_{BZ}\left|M_{cv}(\kappa)\right|^2\delta[\omega_{cv}(k) - \omega]d^3k \quad (11)$$

In equation (11), the integral run over the first Brillion zone, the momentum dipole elements $M_{vk}(k)=<u_{cv}|e\cdot\nabla|u_{ck}>$, where e is the potential vector defining the electric field, are matrix elements for direct transitions between valence-band $u_{vk}(r)$ and conduction-band $u_{ck}(r)$ states corresponding to the transition energy $\hbar\omega_{cv}(k)=E_{ck} - E_{vk}$.

The real part $\varepsilon_1(\varepsilon)$ of the frequency-dependent dielectric function can be derived from the imaginary part using the Kramers-Kronig relation:

$$\varepsilon_1(\omega) = 1 + \frac{2}{\pi}p\int_0^\infty \frac{\omega'\varepsilon_2(\omega')}{\omega'^2 - \omega^2}d\omega' \quad (12)$$

where P implies the principal value of the integral. Based on the knowledge of both real and imaginary parts of the frequency dependent dielectric function, we can calculate important optical functions such as the refractive index $n(\omega)$,optical conductivity function σ, reflectivity, electron energy loss spectra and absorption coefficient using the following expression[44].

$$n(\omega) = \frac{1}{\sqrt{2}}\left[\left\{\varepsilon_1(\omega)^2 + \varepsilon_2(\omega)^2\right\}^{1/2} + \varepsilon_1(\omega)\right]^{1/2} \quad (13)$$

$$k(\omega) = \frac{1}{\sqrt{2}}\left[\left\{\varepsilon_1(\omega)^2 + \varepsilon_2(\omega)^2\right\}^{1/2} - \varepsilon_1(\omega)\right]^{1/2} \quad (14)$$

$$R(\omega) = \left|\frac{\tilde{n}-1}{\tilde{n}+1}\right| = \frac{(n-1)^2 + k^2}{(n+1)^2 + k^2} \quad (15)$$

ISSN: 2319-8753

International Journal of Innovative Research in Science, Engineering and Technology

(An ISO 3297: 2007 Certified Organization)

Vol. 2, Issue 9, September 2013

$$\alpha(\omega)=\frac{4\pi k(\omega)}{\lambda} \quad (16)$$

$$\sigma(\omega)=\frac{2W_{cv}\hbar\omega}{\vec{E}_0^2} \quad (17)$$

Where W_{cv} is the transition probability per unit time.

III. RESULTS AND DISCUSSION

A. *Lattice constant and elastic properties*

We make first-principles calculation to find the most stable structure of BeS, we set a series of different values of lattice constant *a* and calculated the total energy E and the corresponding primitive cell volume V for the ZB BeS. By fitting the calculated energy-volume (E-V) data to the three-order natural strain equation of states EOS [45, 46, 47]

$$E(V)=E_0+\frac{9V_0B_0}{16}\left\{\left[\left(\frac{V_0}{V}\right)^{\frac{2}{3}}-1\right]^3 B_0^{'}+\left[\left(\frac{V_0}{V}\right)^{\frac{2}{3}}-1\right]^2\left[6-4\left(\frac{V_0}{V}\right)^{\frac{2}{3}}\right]\right\} \quad (18)$$

and

$$P(V)=\frac{3B}{2}\left[\left(\left(\frac{V_0}{V}\right)-\left(\frac{V_0}{V}\right)^{\frac{5}{3}}\right)^{\frac{7}{3}}\right]\left\{1+\frac{3}{4}(B_0^{'}-4)\left[\left(\left(\frac{V_0}{V}\right)^{\frac{2}{3}}-1\right)\right]\right\} \quad (19)$$

The structural properties are very important for understanding the solid properties from a microscopic point of view. The reason for this is that the structural properties can provide detailed information about the essential features of inter-atomic binding forces in solids. Our calculated structural properties for ZB BeS at zero pressure are listed in table (1) along with the results of others.

TABLE (1)

LATTICE CONSTANTS a (Å), BULK MODULUS B_0 (GPA) AND ELASTIC CONSTANTS C_{ij} OF ZB BeSAT ZERO PRESSURE WITHIN THE LDA AND GGA

Method		*a*	B	C_{11}	C_{12}	C_{44}
This Works	LDA	4.831804	91.95807	157.1363	59.36895	74.1274
	GGA	4.89	92.50508	156.4544	60.53045	82.43215
Other Works	LDA	4.80[A], 4.811[B] ,4.83[C],	100.8[A], 99.8[B],93[C]	167[A], 165[B], 157[C]	68[A], 68[B], 61[C]	105[A], 85[B], 97[C]
	GGA	4.88[E], 4.88[F],4.861[J]	91.6[E], 93.1[F],96.03[J]	153.7[E], 158.2[F], 155.14[J]	60.6[E], 61.1[F],61.45[J]	110.7[A], 92.7[F],81.6[J]
Experimental		4.87[D]				

[A]FROM REF. [30],[B]FROM REF. [28],[C]FROM REF. [49],[D]FROM REF. [48],[E]FROM REF. [8],[F]FROM REF. [12],[J]FROM REF. [27]

Table (2) shows the variation of the lattice constant *a*, elastic constants C_{ij}, bulk modulus *B*, Young modulus E and Poisson ratio γ with pressures *P* for BeS in the ZB structure within the (2.A) LDA and (2.B) GGA. It is well known that a cubic crystal such as zinc-blende structure has only three independent elastic constants, namely C_{11} , C_{12} and C_{44} ,which are reported to be related to the second-order change in the internal energy of a crystal under deformation . The mechanical stability criteria for a cubic crystal are given by [21]

C_{11} - C_{12}›0 ,C_{11}›0 , C_{44}›0, C_{11} +2 C_{12}›0

Hence to investigate the stability of BeS we have calculated the elastic constants under hydrostatic pressure using the ab-initio stress-strain relations, where the stress is calculated as a function of the strain with the internal coordinates optimized under each strain condition and the elastic constants are the derivates of the stress with respect to the strain. The bulk moduli from the total energy minimization and from the elastic constants have nearly the same value, for both GGA and LDA approximations. This may be an estimate of the reliability and accuracy of our calculated elastic constants.

ISSN: 2319-8753

International Journal of Innovative Research in Science, Engineering and Technology

(An ISO 3297: 2007 Certified Organization)

Vol. 2, Issue 9, September 2013

Furthermore, Young, s modulus E, rigidity modulus G_r, and Poisson's ratio γcan be estimated from equations (9) and (10) .
Pressure is known to be a powerful tool to change the properties of a solid. One of the most straightforward ways to study theoretically the pressure effects is to perform the structural optimization, electronic, elastic and optical properties calculations at different hydrostatic pressures.
To study the pressure dependent behavior of the elastic properties of BeS , we mainly focused on the pressure below 100GPa and the calculated pressure dependent results of the LDA and GGA are shown in table 2.A and 2.B, respectively.
From the tables 2.A and 2.B, we can see that C_{11} and C_{12} vary significantly under different pressures in comparison with the variations of C_{44} .Moreover both C_{11} and C_{12} increase monotonically with pressure, whereas C_{44} increases slowly. It is clear from table 2 that the adiabatic bulk modulus B increases rapidly with increasing pressure and show a linear variation with pressure, whereas the Poisson ratio first increases and then decreases slowly. Agreement between the LDA and GGA results can be observed, although LDA underestimates the lattice constants and overestimates the lattice constant and overestimates the elastic constants, whereas GGA overestimates the lattice constant and underestimates the elastic constants. We clearly observe that the elastic constants C_{11}, C_{12} and C_{44}, and bulk modulus B, linearly increase monotonously when pressure is enhanced.

Table 2

THE VARIATION OF THE LATTICE CONSTANT a (Å), ELASTIC CONSTANTS CIJ (GPA), BULK MODULUS B (GPA), YOUNG MODULUS E AND POISSON RATIO Γ, WITH PRESSURES P (GPA) FOR BeS IN THE ZB STRUCTURE WITHIN THE (A) LDA AND (B) GGA.

TABLE 2.A

P	*a*	C_{11}	C_{12}	C_{44}	B	E	γ
0	4.831804	157.1363	59.36895	74.1274	91.95807	124.5766	0.2742
10	4.690528	196.961	96.0328	92.95715	129.6755	134.0088	0.3278
20	4.584924	229.1231	126.3665	98.56825	160.6187	139.2837	0.3555
30	4.500248	265.1462	156.2441	99.3959	192.5448	149.281	0.3708
40	4.429042	296.1026	187.8049	105.2123	223.9041	150.3281	0.3881
50	4.366791	319.1665	213.4757	116.363	248.7059	148.0502	0.4008
60	4.312113	352.9496	240.6182	120.1343	278.062	157.8679	0.4054
70	4.263364	369.3895	268.8894	109.0575	302.3894	142.838	0.4213
80	4.219152	395.1533	285.7667	115.3862	331.7422	136.1679	0.4316
90	4.178801	434.032	323.3435	126.7219	360.2396	157.9443	0.4269
100	4.141724	461.2783	347.8166	133.2832	385.6372	162.237	0.4299

TABLE 2.B

P	*A*	C_{11}	C_{12}	C_{44}	B	E	γ
0	4.89	156.4544	60.53045	82.43215	92.50508	122.683	0.279
10	4.739438	191.4974	89.116	93.9908	123.2431	134.8953	0.3176
20	4.627548	226.6115	119.7126	101.7464	155.3455	143.8503	0.3457
30	4.538715	260.0247	150.4624	108.158	186.9832	149.7219	0.3665
40	4.464568	289.5924	178.1744	111.935	215.3137	153.8577	0.3809
50	4.400767	317.2145	208.8313	116.9015	244.959	151.4096	0.397
60	4.344707	351.8757	232.8057	118.617	272.4957	166.4808	0.3982
70	4.294649	375.6508	261.6176	120.6349	299.6286	160.8472	0.4105
80	4.249433	402.8401	287.7895	122.4598	326.1397	162.9929	0.4167
90	4.208	422.1865	316.1153	122.5435	351.4723	151.4872	0.4282
100	4.169904	451.6927	341.0651	122.2695	377.9409	158.2225	0.4302

B. Electronic properties

For the ZB ofBeS, the calculated electronic band structure (left panel)and the totaldensity of state (TDOS) (right panel) along the various symmetry lines at 0 GPa and 60 GPaareillustrated in Figs.1(a) and 1(b), from which we can see that the top of valence band (VB) is at G-symmetry point and the bottom of conduction band (CB) is at X-symmetry point, which suggests that the ZB

ISSN: 2319-8753

International Journal of Innovative Research in Science, Engineering and Technology

(An ISO 3297: 2007 Certified Organization)

Vol. 2, Issue 9, September 2013

BeS has an indirect gap occurring between G and X points. Figure 1(a) shows that at 0 GPa, the indirect band gap (G_V - X_C) is 2.911eV, and the minimum direct gap (G_V -G_C) is 5.521eV.The direct and the indirect band gaps together with other theoretical results are present in Table 3. In addition, by comparing the TDOS diagram of Fig.1 (a) with that of Fig.1 (b), we can observe that the TDOS at the edges of the band gap decreases with pressure increasing and the valence band of the ZB BeS shifts upwards while the conduction band shifts downwards. It is also observed that the peaks descend with the pressure increasing but the bandwidths become broad, which implies that the electrons in those states are active under pressure.

TABLE 3

CALCULATED ENERGY GAPS E_G (eV) OF THEZBBeS FOR ZERO PRESSURES

Method	Energy gaps (eV)		
	G_V-G_c	G_V-L_c	G_V-X_c
Present(LDA)	5.521	5.343	2.911
Present(GGA)	5.457	5.838	3.041
Others(LDA)[1]	5.506	5.452	2.828
(LDA)[2]	5.440	5.365	2.912
(GGA)[2]	5.605	4.135	3.192
EV-GGA[1]	6.061	6.108	4.241
Exp.[3].			>5.5

1-(REF.50) 2-(REF.12) 3-(REF.3)

The partial density of states (PDOS) of the ZB BeS at 0 GPa and 60 GPa have been plotted in Figs.2 (a) and 2(b), respectively, where the Fermi level is set to be 0 point. It is seen that at 0 GPa the peaks of PDOS decrease and extend to flat, which suggests that large hole effective masses and some unusual transport properties may be expected for the p-type semiconductor. For the PDOS at 60 GPa, it is observed that the peaks of Be 2s and S 3p increase and extend to high energies, while those of S 3s decreases. This can be understood as that the S 3p and the Be 2s electrons in those states are active under pressure because of the increase of overlap between the bonds and the changed hybridization. In addition, it is clear that the valence band is mainly composed of p electron while the conduction band is composed of the hybrid s and p electrons.

(A)

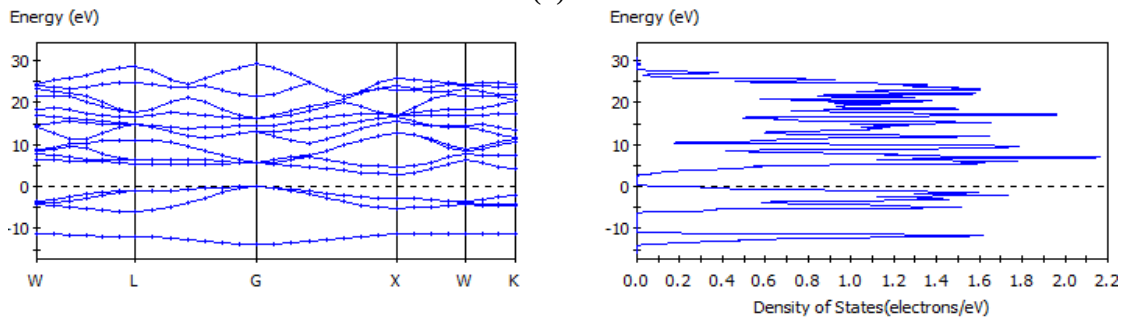

(b)

ISSN: 2319-8753

International Journal of Innovative Research in Science, Engineering and Technology

(An ISO 3297: 2007 Certified Organization)

Vol. 2, Issue 9, September 2013

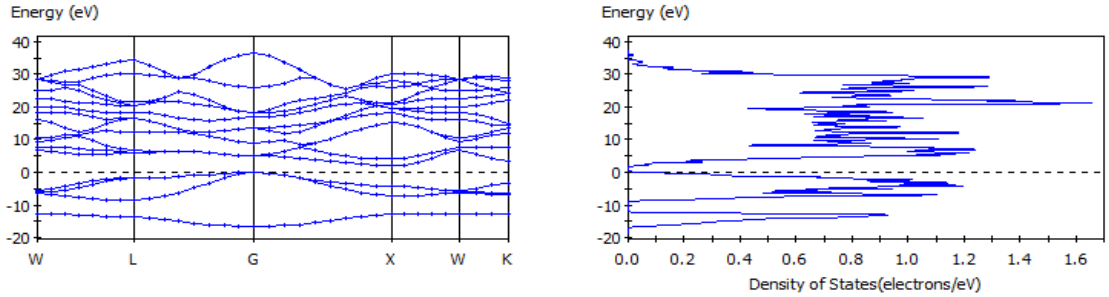

Fig. 1 Band structure and total density of states (TDOS) for ZB –BeS (LDA) along principal symmetrydirections at 0 K (a) 0 GPa, (b) 60 GPa

(a)

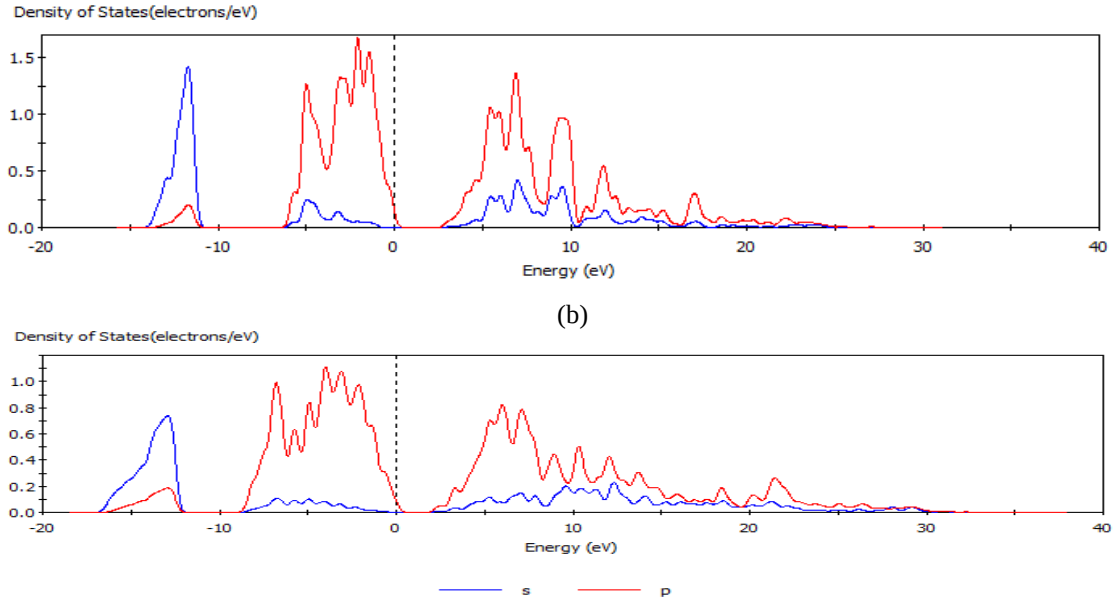

Fig. 2 *Partial density of state (PDOS) of the ZB BeS(LDA)at 0 K: (a) 0 GPa, (b) 60 GPa*

C. Optical properties

In the following, we tackle the frequency-dependentoptical properties of the ZB structured of BeS, and how external pressure influencesthe optical properties. The complex refractive indexNis generallydefined as$N(\omega)=n(\omega)+ik(\omega)$, where theimaginary part$k(\omega)$is related to the absorption coefficientby equation (16). The complex dielectric constantis also related to the complex refractive index by$\varepsilon(\omega)=\varepsilon_1(\varepsilon)+i\varepsilon_2(\omega)$. And the reflectivitycoefficient Ris related to the complex refractiveindex by equation (15). In the present work, the optical properties including dielectric function, absorption equation (16), reflectivity, refractive index, energy-loss function and optical conductivityequation (17) are calculated and analysed.

The absorption coefficient $\alpha(\omega)$ and the reflectivity coefficient $R(\omega)$for the ZB structured of BeS at different pressures are shown in Fig. 3. It is not difficult to observed the existence of two remarkable peaksat about 10.13 and 15.23eV,and that there is almost no absorption at the lower energy region about from 0 to about4eV， This no absorption region means that the material is transparentfrom the partially ultra-violet to the visible lightarea because phonon energy at such range is just within the forbidden

ISSN: 2319-8753

International Journal of Innovative Research in Science, Engineering and Technology

(An ISO 3297: 2007 Certified Organization)

Vol. 2, Issue 9, September 2013

band. The absorption occurs about from4 to 32eV. This absorption region shifts slightly toward high-energy region and the positions of the peaks are as well move towards the higher energy direction with the increase of pressure. For the reflectivity curve, the first or strongest absorption peak takes place around 10.13eV. However, at high-energy region, where photon energy is larger than about 30 eV, the reflection is very weak and slowly goes to zero with increasing photon energy. Obviously, the corresponding relationship for absorption and reflectionspectra is that in the region where absorption is intense, the reflectivity is also larger. That means if a material can strongly absorb light in some regions, it can also effectively reflect light in the same regions. It is clear from Fig. 3, that the shape of the absorptioncoefficient curve is not sensitive to the pressure. However, the positions ofthe peaks are shifted towards lower wavelength.

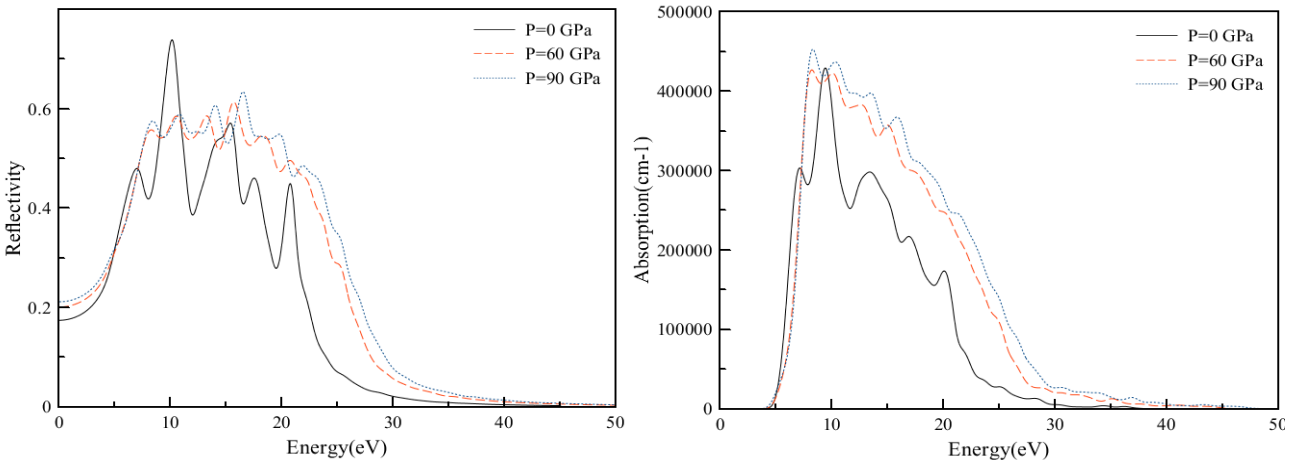

Fig. 3 The absorption and reflectivity curves of ZBBeS at a different external pressure calculatedwith LDA.

The electron energy-loss spectrum L(ω) at normal (solid line) and external pressure (dash dot) are shown in Fig. 4. L(ω) describes the energy loss of a fast electron traversing in a material. From Fig. 4, we can see that there are two prominent peaks in L(ω) spectra which represent the characteristics associated with the plasma resonance. The positions of peaks in the L(ω) spectra also indicatethe point of transition from metallic to dielectric material. Also there is a lossless region from 0 to about 8.0 eV. It can be noticed that just frequencies less than 8.0 eV can be transmitted in ZBBeS

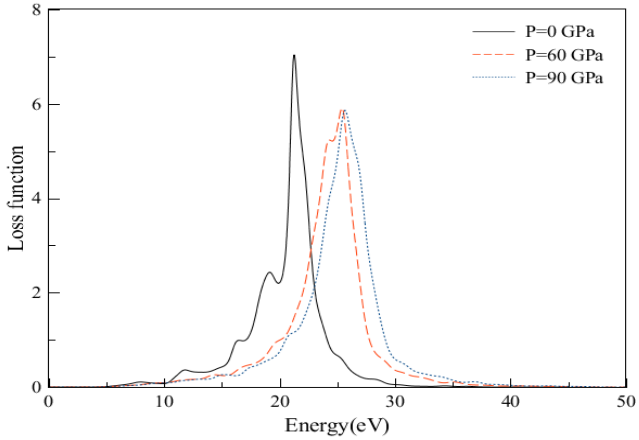

Fig. 4 The loss function curves forZBBeS with LDA at 0GPa(solidline) 60GPa (dashedline)and 90GPa (dottedline).

ISSN: 2319-8753

International Journal of Innovative Research in Science, Engineering and Technology

(An ISO 3297: 2007 Certified Organization)

Vol. 2, Issue 9, September 2013

In Fig.5, we display the (a) dielectric and(b) conductivity function curves for photon energies ranging from 0 eV to 25eV at 0 GPa and 60 GPa separately. It can be seen that in the energy region larger than 20 eV, the values of the imaginary part are very small, while the real part changes very little. In Fig.5a, we display the dielectric function which reflects the band structure of the solid and information about its spectrum .In the real part curve at 0 GPa, there is an obvious peak at 5.54 eV, it is due to the direct interband transitions which originate from the top of the valence band at the L-point to the lowest conduction band. Subsequently, a sharp reduction comes. However, the highest peak in the real part curve decreases with increasing pressure. For the imaginary part of the dielectric function, there also exists such a similar descent, that is, the highest peak in imaginary part curve also decreases with increasing pressure. Many direct or indirect transitions may be found in the band structure with an energy corresponding to the same peak. Thus, the peak in imaginary part $\varepsilon_2(\omega)$.does not correspond to a single interband transition.

In Fig.5b, we display the conductivity function curves. The optical conductivity of a semiconductor is the change in conductivity caused by illumination, either an increase or a decrease. The photoconductive effect is the physical basis of optoelectronic applications of semiconductors. The real part of complex optical conductivity (σ) is shown in Fig.6b. The optical conductivity corresponding to the imaginary part of the dielectric function is also shown in Fig.6b. The real part of complex optical conductivity is zero when the energy is less than 4.3eV and greater than 22.12 eV. It reaches its maximum when energy is 6.58 eV. This is the result of transitions between bands according to the bands and the DOS.

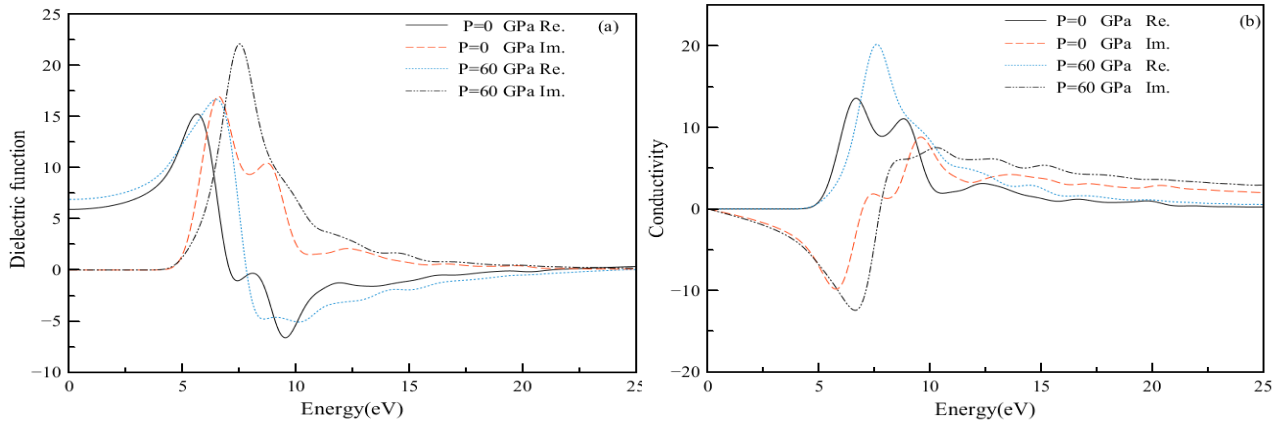

Fig. 5 The real and imaginary part of the (a) dielectric and (b) conductivity function curves forZBBeS with LDA at 0GPaand60 GPa, respectively./

Finally, we study the influence of pressure on the complex refractive index among optical properties for the ZB BeS. In Fig.6, both the real and the imaginary parts of complex refractive index at different pressures are illustrated. It is clearly seen that in a high-energy region, where the frequency of photons is corresponding to the energy larger than 25 eV, the values of the imaginary part are very small, while the values of the real part change very little. This means that the absorption of the high frequency electromagnetic wave is very weak and the refractive index is almost constant in the high frequency region. In low energy region, where the photon energy is less than 5 eV,the imaginary part is almost zero and the real part is almost constant, which suggests that the optical absorption appears mostly in the ultra-violet region, and there are sharp peaks in the low energy area at about 6.85 eV and 9.10 eV, it can be seen that the pressure has little effect on the shape of the refractive index curve, however, the positions of the peaks shift toward higher energies as shown by the arrows in Fig.6.In conclusion, although the positionof these peaks is shifted under pressure, they are still ofthe same type as those at zero pressure.Moreover, the intensityof these main or global peaks is smaller but wider underpressure.

ISSN: 2319-8753

International Journal of Innovative Research in Science, Engineering and Technology

(An ISO 3297: 2007 Certified Organization)

Vol. 2, Issue 9, September 2013

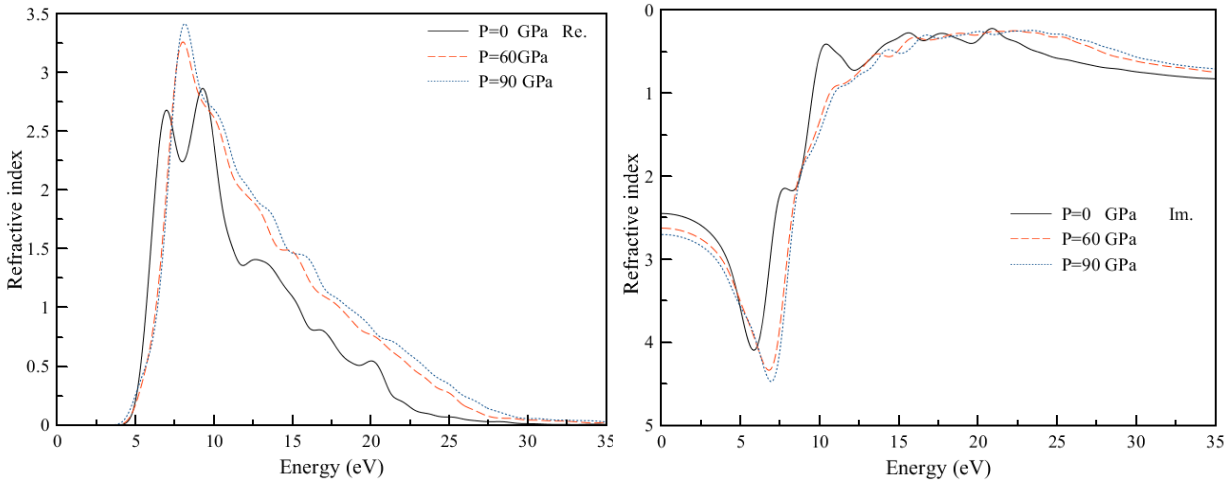

Fig. 6 Real and imaginary refractive index curves at different external pressure conditions for ZBBeS calculated with LDA

IV. CONCLUSIONS

We present the structural, electronic, elastic and optical properties of ZB BeS within the LDA and GGA under pressure by ab-initio pseudopotential density functional method. We found that the ZB structured BeS has indirect gap and the pressure dependence of energy gap has also been obtained. The present results of LDA agree reasonably with GGA calculations, and the properties at zero pressure are in good accordance with available experimental and theoretical values. An indirect band gap induced by the (G- X) transition is presented, with its value being 2.911 eV. The band calculations are comparable very well to available measurements. In addition, we revealed different behaviors of TDOS and PDOS of the ZB BeS under high pressure. The obtained optical parameters, including the dielectric constant, the electron energy loss function, the refractive, conductivity and the absorption indexes, suggest that the strong absorption spectrum appears mostly in the ultra-violet region, and the optical absorption decreases with photon energy in the high energy range.

ACKNOWLEDGMENTS

The author would like to thank Faculty of Science, School of Physics; Duhok University in carrying out computations on the Theoretical Physics Group (TPG) computers.

REFERENCES

[1] B .Bouhafs, H .Aourag, M .Ferhat and M .Certier "Competition between the ionic and covalent character in the series of boron compounds BP, BAs, and BSb"J. Phys.:Condens. Matter 11, 5781 ,1999.
[2] B .Bouhafs, H .Aourag, M .Ferhat and M .Certier, "Trends in band-gap pressure coefficients in boron compounds BP, BAs, and BSb"J. Phys.:Condens. Matter 12, 5655,2000.
[3] W. M. Yim, J .P. Dismukes, E.J. Stofko and R.J. Poff " Synthesis and some properties of BeTe, BeSe and BeS"J. Phys. Chem. Solids 33, 501, 1972
[4] W. Zachariasen. Z. Phys .Chem. (Leipzig) 119(1926)210;W. Zachariasen. Z. Phys .Chem. (Leipzig) 124, 440 ,1926.
[5] C .Narayana, V.J. Nesamony, A.L. Ruoff. "Phase transformation of BeS and equation-of-state studies to 96 GPa"Phys. Rev. B 56, 14338,1997.
[6] H .Luo, K .Chandehari, R.G. Green, A.L. Ruoff, S.S. Trailand, F.J. DiSalvo, et al. "Phase transformation of BeSe and BeTe to the NiAs structure at high pressure"Phys. Rev. B 52, 7058 1995
[7] S. Faraji, A. Mokhtar, "Ab initio study of the stability and electronic properties of wurtzite and zinc-blende BeS nanowires" Phys. Lett. A 374, 3348,2010.
[8] F. El Haj Hassan ,H. Akbarzadeh"Ground state properties and structural phase transition of beryllium chalcogenides" Comput. Mater. Sci. 35, 423,2006
[9] Y. Li, Y.Y.W. Li, Y.M. Ma, T. Cui, G.T. Zou,"High-pressure phase transitions in NiAs-type compounds from first-principles calculations"Phys. Rev. B 81, 052101 ,2010.
[10] Y.X. Cai, R. Xu,"Atomic mechanism of zinc-blende to NiAs high-pressure phase transition in BeTe"J. Phys.: Condens. Matter 20 , 485218. 2008.
[11] A. Berghout, A. Zaoui, J. Hugel,"Fundamental state quantities and high-pressure phase transition in beryllium chalcogenides" J. Phys.: Condens. Matter 18, 10365.2006.

ISSN: 2319-8753

International Journal of Innovative Research in Science, Engineering and Technology

(An ISO 3297: 2007 Certified Organization)

Vol. 2, Issue 9, September 2013

[12] Lei Guo, Ge Hu, Shengtao Zhang, WenjiangFeng, Zhipeng Zhang." Structural, elastic, electronic and optical properties of beryllium chalcogenidesBeX (X = S, Se, Te) with zinc-blende structure" J. Alloy Compd. 561, 16, 2013.
[13] D. Rached, M. Rabah, N. Benkhettou, R. Khenata, "First-principle study of structural, electronic and elastic properties of beryllium chalcogenidesBeS, BeSe and BeTe" Comput. Mater. Sci. 37, 292. 2006.
[14] M. Gonza´ lez-Dı´az, P. Rodrı´guez-Herna´ ndez, A. Muñoz, "Elastic constants and electronic structure of beryllium chalcogenidesBeS, BeSe, and BeTefrom first-principles calculations" Phys. Rev. B 55, 14043.1997.
[15] C.M.I. Okoye, Structural, electronic, and optical properties of beryllium monochalcogenides" Eur. Phys. J. B 39 , 5. 2004.
[16] Imad Khan, Iftikhar Ahmad, D. Zhang, H.A. Rahnamaye Aliabad, S. JalaliAsadabadi. "Electronic and optical properties of mixed Be-chalcogenides" Journal of Phys. and Chem. of Solids 74, 181 ,2013.
[17] N .Munjal, V. Sharma, G. Sharma, V. Vyas, B. K .Sharma, J .E .Lowther. "Ab-initio study of the electronic and elastic properties of beryllium chalcogenidesBeX (X=S, Se and Te)" PhysicaScripta 84,035704.2011.
[18] Y. Huan, C. Jing, Li Zhe, C. Xiang-Rong. "Bottom of Form First-principles calculations for electronic and optical properties of the zinc-blende structured BeS compound under pressure"Chinese Physics B 18,4443. 2009.
[19] K.B. Joshi, R.K. Pandya, R.K. Kothari, B.K. Sharma, "Electronic structure of BeTe and ZnTe"Phys. Status Solidi B 246, 1268.2009.
[20] A. Berghout, A. Zaoui, J. "Hugel, Mechanical stability and deformation potential in beryllium chalcogenides"SuperlatticesMicrostruct. 44, 112,2008.
[21] D. Heciri, L. Beldi, S. Drablia, H. Meradji, N.E. Derradji, "First-principles elastic constants and electronic structure of beryllium chalcogenidesBeS, BeSe and BeTe" Comput. Mater. Sci. 38, 609.2007.
[22] Z. Mameri, A. Zaoui, A. Belabbes, M. Ferhat, Mater. "Pressure effects on the phonon modes in beryllium chalcogenides "Chem. Phys. 123,343. 2010.
[23] V. Wagner, J.J. Liang, R. Kruse, S. Gundel, M. Keim, "Lattice Dynamics and Bond Polarity of Be-Chalcogenides A New Class of II-VI Materials ,Phys. Status Solidi B 215, 87,1999.
[24] S. Doyen-Lang, O. Pages, L. Lang, J. Hugel, "Phonon Dispersion Curves of BeSe and BeTe"Phys. Status Solidi B 229, 563.2002.
[25] V. Wagner, S. Gundel, J. Geurts, T. Gerhard, T. Litz, H.-J. Lugauer, F. Fisher, A. Waag, G. Landwehr, R. Kruse, C. Beker, U. Kuster, "Optical and acoustical phonon properties of BeTe"J. Cryst. Growth 184/185, 1067.1998.
[26] F.J. Kong, G. Jiang, "Phase transition, elastic, thermodynamic properties of zinc-blend BeSe from first-principles"Physica B 404, 3935 ,2009.
[27] Chang Jing, Chen Xiang-Rong, Zhang Wei, Zhu Jun."First-principles investigations on elastic and thermodynamic properties of zinc-blende structure BeS" Chinese Physics B 17, 1377 ,2008.
[28] S. Saib, N. Bouarissa, "Ground-state and lattice dynamical properties of BeS in the zinc-blende and nickel arsenide phases"Solid State Sci. 12, 563. 2010.
[29] P.S. Yadav, R.K. Yadav, S. Agrawal, B.K. Agrawal, "Ab initio study of electronic and optical properties of Be-chalcogenides in GW approximation"Physica E 36, 79,2007.
[30] R. Khenata, A. Bouhemadou, M. Hichour, H. Baltache, "Elastic and optical properties of BeS, BeSe and BeTe under pressure"Solid-State Electronics. 50, 1382,2006.
[31] M. Ameri, D. Rached, M. Rabah, F. El Haj Hassan, R. Khenata, M. Doui-Aici, "First principles study of structural and electronic properties of BexZn1−xS and Bex Zn1−xTealloys"Phys. Status Solidi B 245, 106 ,2008.
[32] F. El Haj Hassan, "First-principles calculations on the origins of the gap bowing in BeSxSe1-x, BeSxTe1-x and BeSexTe1-x alloys"Phys. Status Solidi B 242, 909,2005.
[33] S. Kumar, Tarun K. Maurya, S. Auluck," Electronic and optical properties of ordered BexZn1−xSe alloys by the FPLAPW method" J. Phys.: Condens. Matter 20, 075205 ,2008.
[34] S. Kumar, Tarun K. Maurya, S. Auluck, :" Optical properties and critical points of BexZn1-xSe alloys "J. Alloy Compd. 480, 717,2009.
[35] S. Abdi-Ben Nasrallah, S. Ben Afia, H. Belmabrouk,"Optoelectronic properties of zinc blende ZnSSe and ZnBeTe alloys" Eur. Phys. J. B 43,3,2005.
[36] A. Muñoz, P. Rodrı´guez-Herna´ ndez, A. Mujica, "Ground-state properties and high-pressure phase of beryllium chalcogenidesBeSe, BeTe, and BeS"Phys. Rev. B 54, 11861,1996.
[37] S. J. Clark, Matthew D. SegallII, Chris J. PickardII, Phil J. HasnipIII, Matt I. J. ProbertIV, Keith RefsonV and Mike C. PayneII and Mike C. PayneII "First principles methods using CASTEP"Z. Kristallogr. 220, 567,2005.
[38] M.C. Payne, M.P. Teter, D.C. Allan, T.A. Arias, J.D. Joannopoulos, "Iterative minimization techniques for ab initio total-energy calculations: molecular dynamics and conjugate gradients"Rev. Mod. Phys.64, 1045,1992.
[39] D. Vanderbiltm"Soft self-consistent pseudopotentials in a generalized eigenvalue formalism"Phys. Rev. B 41, 7892.1990.
[40] D.M. Ceperly, B.J. Alder, "Ground State of the Electron Gas by a Stochastic Method"Phys. Rev. Lett. 45, 566,1980.
[41] J.P. Perdew, A. Zunger, "Self-interaction correction to density-functional approximations for many-electron systems"Phys. Rev. B 23, 5048,1981.
[42] J.P.Perdew, K. Burke, M. Ernzerhof, "Generalized GradientApproximation Made Simple"Phys. Rev. Lett. 77,3865., 1996.
[43] E .Schreiber, OL .Anderson, N .Soga. "Elastic constants and their measurement". New York: McGraw-Hill; 1973.
[44] C. Amrosch-Draxl, J.O.Sofo Linear optical properties of solids within the full-potential linearized augmented planewave method. omput. Phys. Commun. 175,1,2006.
[45] F. Birch," Finite Elastic Strain of Cubic Crystals"Phys. Rev. 71, 809 1947.
[46] B.H.Elias,N.S.Saadi, "First Principle Pseudopotential Study of Zinc Blend to Rock Salt Phase Transition in ZnS"International Journal of Scientific & Engineering Research,, 4,2,1,2013.
[47] B.H.Elias, "Elastic and Electronic Properties and the (B3-B1) Phase Transition of ZnO"International Journal of Scientific & Engineering Research,.4,5,295,2013.
[48] N. Victor Jaya, in: Proceedings of the IV National conference on High Pressure Science and Technology, Scp. 11-13, IGCAR, Kalpakkam, India, 1997.
[49] S. Laref ,A. Laref, "Thermal properties of BeX (X = S, Se and Te) compounds fromab initio quasi-harmonic method" Comput. Mater. Sci.51,135, 2012.

ISSN: 2319-8753

International Journal of Innovative Research in Science, Engineering and Technology

(An ISO 3297: 2007 Certified Organization)

Vol. 2, Issue 9, September 2013

[50] Y. Al-Douri, H. Baaziz, Z. Charifi, Ali H. Reshak, "Density functional study of optical properties of beryllium chalcogenides compounds in nickel arsenide B8 structure" Physica B 407, 286 ,2012.

BIOGRAPHY

Dr.BadalHayder Elias is an Assistant Professor in Theoretical Physics. His Post Graduate specialization is Theoretical Physics. He obtained his Ph.D. degree in the field of Atomic Physics. He has more than 20 research publication in the areas of density functional theory and Quantum Scattering.